



Estimating spatial variability of baseline isoscapes from fish isotopic signatures at the community level

J.J. Ortiz^{a,*}, I. Preciado^a, M. Hidalgo^b, J.M. González-Irusta^a, I.M. Rabanal^a, L. López-López^a

^a Spanish Institute of Oceanography (IEO-CSIC), C.O. Santander, Av. de Severiano Ballesteros, 16, 39004 Santander, Cantabria, Spain

^b Spanish Institute of Oceanography (IEO-CSIC), C.O. Baleares, Muelle de Poniente, s/n, 07015 Palma, Balearic Islands, Spain

ARTICLE INFO

Keywords:

Fish community
Demersal
GAMs
Isotopic baseline
Linear mixed-effects models
Stable Isotopes
Trophic ecology

ABSTRACT

One of the main limitations in the application of stable isotopes to marine trophic ecology is obtaining a reliable baseline upon which to calculate isotopic enrichment. Isotopic baselines are variable in space and time, influenced by several environmental factors such as terrestrial runoff, oceanic currents or primary production, and thus, investigating their patterns of variability is essential to gain confidence in the estimates of trophic position based on isotopic signatures. We here propose a multispecies and multitrophic approach to study baseline isoscapes for nitrogen ($\delta^{15}\text{N}$) and carbon ($\delta^{13}\text{C}$), which we test on the demersal community of the Northwestern Iberian Peninsula. Using a set of 372 isotopic data of 11 demersal fish species sampled during autumn, we modelled the spatial variability of the isotopic baseline (for $\delta^{15}\text{N}$ and $\delta^{13}\text{C}$ separately) by removing the biological effect of species identity and individual length. Using the residuals of these models, which represent the isotopic baseline anomalies, we investigated the effect of environmental variables in driving the observed spatial patterns. Our results identify clear and consistent spatial patterns for the $\delta^{13}\text{C}$ isotopic baseline. This isoscape achieved the lowest values in the westernmost part of the study area (Galician coast) increasing towards the east (Cantabrian Sea). This spatial pattern was mostly driven by primary production and organic matter in the sediment, reflecting the influence of upwelling intensity in the $\delta^{13}\text{C}$ isotopic baseline over the study area. Baseline isotopic anomalies of $\delta^{15}\text{N}$, on the other hand, did not show clear spatial patterns, suggesting that for this isotopic baseline spatial patterns at the regional scale might not be as consistent. Our study brings forward the potential of multispecies isotopic data for approximating the environmental isotopic baselines for the whole ecosystem.

1. Introduction

Research on marine trophic ecology is increasingly relying on stable isotope analysis (SIA) to investigate food web structure, functioning and connectivity (e.g. McMahon et al., 2013; Jennings and Warr, 2003; Tanaka et al., 2010; MacKenzie et al., 2011). These analyses, most commonly based on isotope ratios of N ($^{15}\text{N}/^{14}\text{N}$) and C ($^{13}\text{C}/^{12}\text{C}$), inform both of the trophic position and the source of the main trophic pathways for consumers (Layman et al., 2011). Using this method, researchers have been able to capture fluctuations in food sources and their limitations (Fischer, 1991; Rau et al., 1991; Jennings and Warr, 2003; Barnes et al., 2009), the trophic position on the food web (Post, 2002; Lorrain et al., 2015) and the spatial movement of animals along their migration's routes (e.g. Tanaka et al., 2010; MacKenzie et al., 2011). The interpretation of SIA results of biological organisms,

however, rely on our understanding of the species metabolism and isotopic fractionation (Elsdon et al., 2010), the transfer efficiency along the different food web levels (McMahon et al., 2015) and ultimately, the underlying isotopic baselines together with the factors that shape this so called isoscapes (Hussey et al., 2014). However, characterising these isoscapes is particularly challenging in the marine environment due to its highly dynamic nature (Post, 2002; Elsdon et al., 2010; Ohshimo et al., 2019), which also complicates understanding biogeochemical cycling at small scales (e.g. Graham et al., 2010; Trueman et al., 2012).

Intuitively, environmental samples of carbon and nitrogen could be thought of as the most straightforward method to measure isoscapes. However, the isotopic signatures of environmental samples are highly variable at the small scale and thus, might not represent the space-time scales that predators integrate within their dynamics, home ranges and life cycles. While particulate organic matter filtered from the water

* Corresponding author.

E-mail address: juanjose.ortiz@ieo.csic.es (J.J. Ortiz).

<https://doi.org/10.1016/j.pocean.2024.103205>

Received 27 September 2023; Received in revised form 10 January 2024; Accepted 14 January 2024

Available online 22 January 2024

0079-6611/© 2024 The Author(s). Published by Elsevier Ltd. This is an open access article under the CC BY license (<http://creativecommons.org/licenses/by/4.0/>).

column (POM) and organic matter obtained from sediment samples (SOM) are often used in the literature (e.g. Tاملander et al., 2009; Bosman et al., 2020; Ho et al., 2021), researchers are increasingly establishing the baselines at the consumer level to homogenize this high environmental variability. Thus, the first trophic levels of food webs are commonly used, estimating the isotopic baselines based on phytoplankton (e.g. Magozzi et al., 2017), zooplankton (Espinasse et al., 2022), or primary consumers such as grazers and filter-feeders (Post, 2002; Vokhshoori et al., 2014). In fact, higher trophic levels such as forage fish and squids (Ohshimo et al., 2019) or gelatinous carnivores (MacKenzie et al., 2014; St. John Glew et al., 2019) can also be used to obtain valid estimates of the isotopic baselines. Some approaches have generated isoscapes using different trophic levels within an ecosystem (e.g. POM, primary producers, primary and secondary consumers) which have proven comparable among them, despite the dynamic enrichment they undergo when moving up within the trophic web (Lorrain et al., 2015).

In this study we propose, for the first time to our knowledge, using a biological fish community as a multi-species data source for isoscapes estimation. We test this approach with data from the marine ecosystem over the North Atlantic coast of Spain. The North Atlantic is among the most studied marine ecosystems of the planet (Espinasse et al., 2022), but poorly studied in terms of SIA models (McMahon et al., 2013). Specifically, within the North Atlantic coast of Spain, stable isotopes have been widely used to study the trophic ecology of a wide range of marine organisms (e.g. González-Irusta et al., 2014; Preciado et al., 2017; Iglesias et al., 2023), using different environmental and biological samples to correct for the isotopic baselines. With our approach we aim to estimate isoscapes for a wide demersal fish community obtaining reliable baseline estimates which integrate the pelagic and benthic feeding resources this community relies on. In addition, we aim to identify the main environmental factors driving the spatial patterns observed in these baseline isoscapes. As a result, we expect this approach to increase our understanding of isotopic baselines estimation in predator communities which rely on different basal resources within a marine food web.

2. Materials and methods

2.1. Study area

The study area comprehends the continental shelf of the North-Atlantic coast of Spain, i.e. the southern Bay of Biscay. The geomorphology of this area is characterized by a narrow continental shelf on which a large number of small rivers discharge, not contributing significantly to the local oceanography (Gil, 2008). Oceanographic patterns in this area tend to be seasonal and highly variable; the poleward current predominates in intermediate waters during autumn–winter (Decastro et al., 2011) while upwelling phenomena caused by westerly winds predominate during summer, decreasing its intensity from West to East within the study region (Gil, 2008; Alvarez et al., 2011; López-López et al., 2017a). The narrow continental shelf along with the upwelling phenomena, which enhance primary production (Tenore et al., 1995), promote the development of a complex and diverse ecosystem with a well-structured food web (López-López et al., 2017b).

2.2. Stable isotope analysis: Sample collection and laboratory protocol

Specimens were obtained by bottom trawling onboard oceanographic surveys DEMERSALES (ICES code: SPGFS WIBTS-Q4) carried out annually during early autumn (September–October) to study the benthic-demersal communities in the North-Atlantic coast of Spain (Sánchez and Serrano, 2003). Specifically, stable isotope analyses were performed in non-consecutive years 2010, 2012, 2013, and 2020 covering the continental shelf and upper slope of the study area with 71

sampling stations between 58 and 580 m depth (Fig. 1).

In each station, and after identifying the full catch to the species level, three specimens of each target species were randomly selected for subsequent trophic analyses (Table 1). For each of these specimens, we measured total length (cm) and dissected 1 cm³ of white muscle from the anterior dorsal area carefully removing any tissue other than muscle attached to the sample (such as skin, scales or blood). The muscle sample was stored at –20 °C until further processing in the lab.

Additionally, environmental samples of particulate organic matter (both in the water column, POM and in the sediment SOM) were collected aboard these surveys at some of the stations where fish sampling was performed. POM samples were obtained from subsurface water (approx. 5 m depth), filtered through 200 µm mesh to eliminate large particles that could bias the measures, and then filtered through a pre-combusted Whatman GF/F until clogged and freeze stored at –20 °C. Sediment samples were collected using a sediment collector attached to the ground rope of the trawl and freeze stored at –20 °C on board.

In the laboratory, muscle samples were thawed and dried for 48 h at 60 °C. Dry samples were then grounded to a fine powder using a hand mortar and pestle. Environmental samples (POM and SOM) were divided into two equal fractions, one of them being directly dried, as the muscle samples for δ¹⁵N analyses, and the other half being acidified to dissolve inorganic carbon for measuring δ¹³C (see López-López et al., 2017b for further details) and processed afterwards as described below.

Subsamples of these powdered samples were weighed to the nearest µg and placed into tin capsules for subsequent δ¹³C and δ¹⁵N determinations. Isotopic analyses were performed at the Laboratorio de Isótopos Estables (LIE-EBD, Spain; <https://www.ebd.csic.es/lie/index.html>), Estación Biológica de Doñana, CSIC, certified to ISO9001:2015 and ISO14001:2015 quality and environmental management systems, and at the Scientific-Technical Service of the University of the Balearic Islands. All samples were analysed using an isotope-ratio mass spectrometry system via coupled conflow interface with international standards. The isotopic composition was reported in the conventional delta (δ) per mil notation (‰), relative to Vienna Pee Dee Belemnite (δ¹³C) and atmospheric N₂ (δ¹⁵N). Replicate assays of standards routinely inserted within the sampling sequence indicated analytical measurement errors of ± 0.1‰ and ± 0.2‰ for δ¹³C and δ¹⁵N, respectively.

2.3. Estimate of isotopic baselines- model description

In order to obtain the environmental isotopic baseline, we developed models which could single out the underlying environmental signal embedded in all the animal samples. To do this, we considered the main biological factors of variability in the isotopic signal, which mostly pertain to the species identity and the individual size (Galvan et al., 2010; MacKenzie et al., 2014; Ohshimo et al., 2019). We modelled the isotopic signature as a nested response of individual length for each of the species using Linear Mixed-Effects Models (Harrison et al., 2018), including sampling year as a random effect. The resulting models (δ¹³C and δ¹⁵N), were chosen as the first step in the study:

$$\delta^{13}\text{C} \text{ or } \delta^{15}\text{N} \sim \text{lmer}(\text{Length} + (1 + \text{Length}|\text{Species}) + (1|\text{Year}))$$

“lmer” function of the “lme4” package of R (Bates et al., 2015) to fit the Linear Mixed-Effects Models, where isotopic values are influenced by a fixed effect variability (Length), and by additional variability modelled through random effects, including both the random variation of length dependent on species (1 + Length|Species) and the constant random effect of year (1|Year). The improvement of the model following the addition of these random effects was evaluated by comparing the results of model with those of a null model, in which these effects were not included, using ANOVA function of package “stats” (R Core Team, 2022).

The residuals obtained from these multispecies models, reflected the

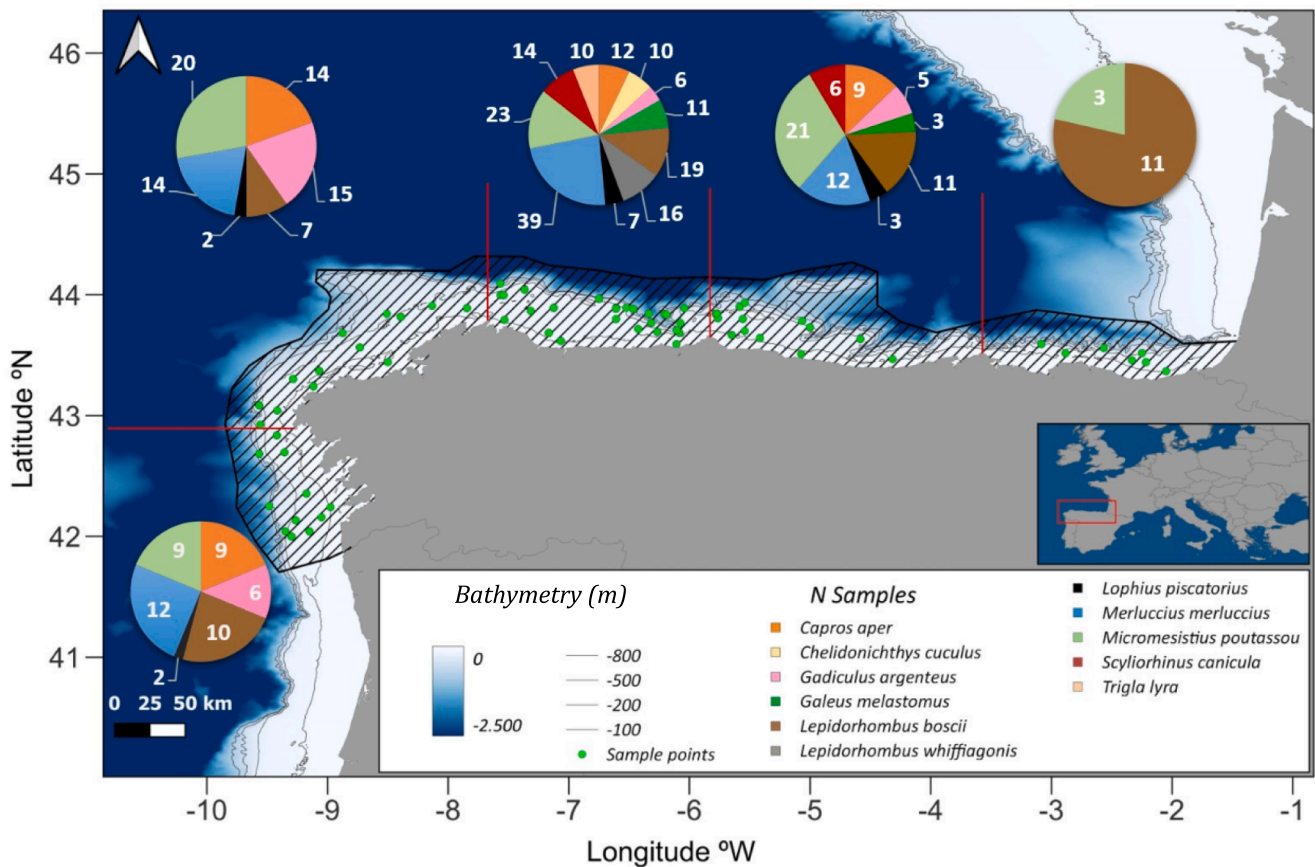


Fig. 1. Study area, sample points and number of samples of each species, distributed by five sampling zones. * The separation into subareas is only effective for the visualisation of the data distribution. Data are treated as a whole, without using these sub-areas for the study.

Table 1

List of fish species sampled showing total number of specimens analysed (n), length range (cm), geographic position and isotopic signatures of $\delta^{13}\text{C}$ and $\delta^{15}\text{N}$ (minimum and maximum values).

Species	n	Length (cm)		Latitude °N		Longitude °W		$\delta^{13}\text{C}$ (‰)		$\delta^{15}\text{N}$ (‰)	
		Min	Max	Min	Max	Min	Max	Min	Max	Min	Max
<i>Capros aper</i>	44	5	9	41.99	43.99	-5.00	-9.36	-20.30	-17.9	11.00	12.20
<i>Chelidonichthys cuculus</i>	10	19	28	43.68	44.04	-7.12	-7.53	-19.74	-18.72	11.17	12.20
<i>Gadiculus argenteus</i>	32	6	9	42.13	43.99	-5.00	-9.28	-19.6	-17.7	9.90	11.10
<i>Galeus melastomus</i>	14	29	47	43.84	43.97	-4.58	-6.47	-19.96	-17.84	10.69	11.70
<i>Lepidorhombus boscii</i>	59	11	75	42.92	43.97	-5.07	-9.57	-19.55	-16.92	9.99	12.81
<i>Lepidorhombus whiffiagonis</i>	16	14	43	43.68	43.97	-7.12	-7.17	-19.80	-17.85	9.94	11.79
<i>Lophius piscatorius</i>	14	19	86	42.68	44.09	-5.07	-9.57	-18.53	-17.49	11.67	15.94
<i>Merluccius merluccius</i>	77	10	56	41.99	43.99	-5.00	-9.36	-20.60	-17.69	9.55	13.46
<i>Micromesistius poutassou</i>	76	13	41	42.35	43.97	-5.00	-9.57	-19.76	-17.90	8.80	13.18
<i>Scyliorhinus canicula</i>	20	19	51	43.59	43.77	-6.07	-7.07	-18.74	-17.32	10.57	12.71
<i>Trigla lyra</i>	10	10	33	43.68	43.97	-7.12	-7.17	-19.16	-18.13	11.58	12.41
Total	372										

variability in the isotopic signatures that could not be explained by biological variables (species and individual size) and, as such, the part of the variability that could be assumed as baseline isoscapes of $\delta^{13}\text{C}$ and $\delta^{15}\text{N}$.

The isotopic signatures of environmental samples (POM and SOM), were compared with the baseline estimates obtained from the previous models. We performed a pair-wise correlations analyses between POM and SOM isotope data and the residuals of the first $\delta^{13}\text{C}$ and $\delta^{15}\text{N}$ linear mixed models at the same geographical location.

2.4. Environmental drivers of the isotopic baselines - variables and model description

In a second step, we used several environmental variables to explain the spatial patterns observed in the isotopic baseline estimates. These environmental variables were identified from the scientific literature as those commonly influencing isotopic baselines and were generally related to primary production, hydrodynamics, depth and sediment type. Sediment type (relative granulometry and organic matter content) and primary production (chlorophyll-a) were considered as potential explanatory variables for both $\delta^{13}\text{C}$ and $\delta^{15}\text{N}$ baselines (Bode et al., 2007; Post, 2002; Vokhshoori et al., 2014; Ohshimo et al., 2019). Depth was also considered a potential driver of the isoscapes for both isotopes,

as it could serve as a proxy for several other variables with direct physiological impact on biological processes, such as light pressure or food availability (Nerot et al., 2012). Additionally, few variables were only considered as potential drivers of the $\delta^{13}\text{C}$ baseline, as they could explain organic matter fluctuations (Puig et al. 2001). These were terrigenous carbon input, related to distance to coast and hydrodynamics, including both waves and tides (Waite et al., 2007; Vokhshoori et al., 2014; Ishikawa et al., 2021). It should be noted that, since all data were sampled in autumn, seasonality was not considered as an explanatory variable, and environmental variables refer to annual means (see details in supplementary Table C). These environmental variables were obtained as raster layers from different sources at different resolutions (Supplementary C; D), and resized to 3x3 km resolution grids by linear interpolation with the “projectRaster” function of the “raster” package of R (Hijmans et al., 2021). Moreover, the temporal scale of the environmental layers has been adjusted (when possible) to that of our data, specifically for dynamic environmental variables such as chlorophyll-a. From these final environmental rasters we have extracted the own values for each of our sampling points, according to the years of the data.

After having inspected the correlation (r) between the initial 9 environmental variables: Chlorophyll-a (Chl, mg/m³), Q50 (substrate mean grain diameter, μm), Fine sand (substrate fine sand %), Mud (substrate mud %), Coarse sand (substrate coarse sand %), Organic matter (OM, substrate organic matter %), Hydrodynamic energy (currents and waves additive effect, m/s), Coast distance (km from sampling location to coast) and Depth (m). We removed those with values over 0.7 (maximum allowed threshold), finally retaining 6 variables for further analyses based on its higher ecological relevance: Chlorophyll-a, Mud, Coarse sand, Organic matter, hydrodynamic energy and Depth. The initial GAM models were specified as follows:

$$\delta^{13}\text{C} \sim \text{GAM}(s(\text{Chl}, k = 4) + s(\text{Mud}, k = 4) + s(\text{Coarse sand}, k = 4) + s(\text{OM}, k = 4) + s(\text{Hydrodynamic energy}, k = 4) + s(\text{Depth}, k = 4))$$

$$\delta^{15}\text{N} \sim \text{GAM}(s(\text{Chl}, k = 4) + s(\text{Mud}, k = 4) + s(\text{Coarse sand}, k = 4) + s(\text{OM}, k = 4) + s(\text{Depth}, k = 4))$$

where “s” represents the smoothing class, cubic splines, and “k” is the fixed number of knots for each smoother. The significance of the covariates is shown in Table 2.

Finally, in order to select the best gam model for each isotope, we applied the “dredge” function, package “MuMIn” (Bartoń, 2022), that performs random combinations of all the explanatory variables included in the initial GAM models. Thus, we obtained the combination of variables (significant or not) that gave us the best model based on generalized cross validation (GCV), deviance explained and Akaike Information Criterion, AIC (Akaike, 1974) of the GAMs. The spatial correlation of the model residuals was checked using Variograms and Moran Test. All statistical analyses were performed in R version 4.2.2 (R

Table 2

Results of the Generalised Additive Models performed for $\delta^{13}\text{C}$ and $\delta^{15}\text{N}$ isotopic baseline. Degrees of freedom (df), χ^2 , p-value and statistical significance of the explanatory variables of each GAM model are shown.

Environmental Variables	$\delta^{13}\text{C}$ GAM Model				
	df	χ^2	P	Deviance explained	Total Deviance explained
Hydrodynamic energy	4.73	2.78	0.15	0.82%	30.2%
Chla	95.90	1.00	0.00	12.47%	
Coarse Sand	4.43	1.89	0.12	0.85%	
Depth	4.71	2.70	0.16	0.90%	
OM	6	1.00	0.01	0.87%	
	$\delta^{15}\text{N}$ GAM Model				
Depth	5.02	2.82	0.14	1.50%	4.04%
Mud	2.53	1.00	0.11	1.56%	
OM	5.83	2.32	0.06	2.55%	

Core Team, 2022) using the packages “stats”, “lme4” (Bates et al., 2015), “mgcv” (Wood, 2011), “MuMIn”.

3. Results

3.1. Stable isotope results

The pool of 372 samples comprised 11 species of fish (9 Teleostei and 2 Elasmobranchii, Fig. 1), representing a wide range of trophic positions in the benthic-demersal fish community and the species’ size distribution within the catch.

The isotopic signatures of these species reflected the width of the fish community analysed. Community values of $\delta^{13}\text{C}$ ranged between -20.6 and -16.92 (belonging to *Merluccius merluccius* and *Lepidorhombus boscii*, respectively), while $\delta^{15}\text{N}$ ranged between 8.80 and 15.94 (belonging to *Micromesistius poutassou* and *Lophius piscatorius*, respectively) (Table 1).

Regarding the environmental data, $\delta^{13}\text{C}$ ranged between -29.99 and -23.58 ‰ in sediment samples (SOM) and between -26.9 and -19.83 ‰ in particulate organic matter in the water column (POM), with lower values to the west and higher values to the east of study area. Moreover, $\delta^{15}\text{N}$ ranged between 3.46 and 7.3 ‰ in SOM (spatially more homogeneous) and between 1.8 and 7.7 ‰ in POM (more spatially variable) (Supplementary A; B).

3.2. Modelling baseline isoscapes

The linear mixed-effects models explained a large proportion of the variance of the community $\delta^{13}\text{C}$ and $\delta^{15}\text{N}$ isotopic signatures, validating our approach to model individual length nested within species identity. Both models identified a generalised positive trend of the isotopic signature values along individual size ($t = 7.382$, d.f. = 8.25, $p < 0.001$ in the $\delta^{15}\text{N}$ model and $t = 5.481$, d.f. = 9.16, $p < 0.001$ in the $\delta^{13}\text{C}$ model). In addition, the effect of length by species, was stronger for $\delta^{15}\text{N}$ (Fig. 2A) than for $\delta^{13}\text{C}$, but significant in both cases ($\chi^2 = 207.77$, d.f. = 3, $p < 0.001$ and $\chi^2 = 94.22$, d.f. = 3, $p < 0.001$, respectively). Year was only significant in the $\delta^{13}\text{C}$ model ($\chi^2 = 12.72$, d.f. = 1, $p < 0.001$), but was included in the $\delta^{15}\text{N}$ model nevertheless ($\chi^2 = 1.35$, d.f. = 1, $p = 0.246$). The species-specific trends were also quite uniform in the $\delta^{15}\text{N}$ model, with exception of *Merluccius merluccius* which displayed a notoriously steeper trend with size. Within the $\delta^{13}\text{C}$ model, species-specific trends of the isotope along the size range of the community were more variable, but positive in all cases (Fig. 2B). No significant anisotropy was observed in either $\delta^{13}\text{C}$ and $\delta^{15}\text{N}$ residuals, which accounted for 41.6% and 21.7% of the variability, respectively.

The residuals from these models, after removing the biological signal of individual size and species identity, were assimilated as the anomalies of the baseline isotopic signature in the benthic-demersal fish community. The wide coverage of the sampling sites allowed us to obtain a highly resolved insight into the spatial variability of the residuals over the study area (Fig. 3;4).

The isotopic baseline for $\delta^{13}\text{C}$ displayed the most negative anomalies in the westernmost area, and particularly near the coast (Fig. 3). On the contrary, the most positive anomalies appeared in the eastern half of our study area, however some patches of weak anomalies were found close to the coast and to the French border. The isotopic baseline for $\delta^{15}\text{N}$ did not show such strong spatial patterns in the anomalies (Fig. 4). The distribution seemed more homogeneous, and no strong geographical zonation could be distinguished. Most of the anomalies showed neutral or slightly positive values, with few exceptions of positive data that suggest some discontinuities and few negative focal points.

Comparing the baseline isoscapes with the isotopic values directly measured in environmental samples (POM and SOM), we did not identify any significant correlation (Pearson’s correlation) for $\delta^{13}\text{C}$ or $\delta^{15}\text{N}$ ($\delta^{13}\text{C}:\text{POM} = 0.057$; $\delta^{13}\text{C}:\text{SOM} = 0.234$ - $\delta^{15}\text{N}:\text{POM} = 0.072$; $\delta^{15}\text{N}:\text{SOM} = 0.001$) (Supplementary A; B).

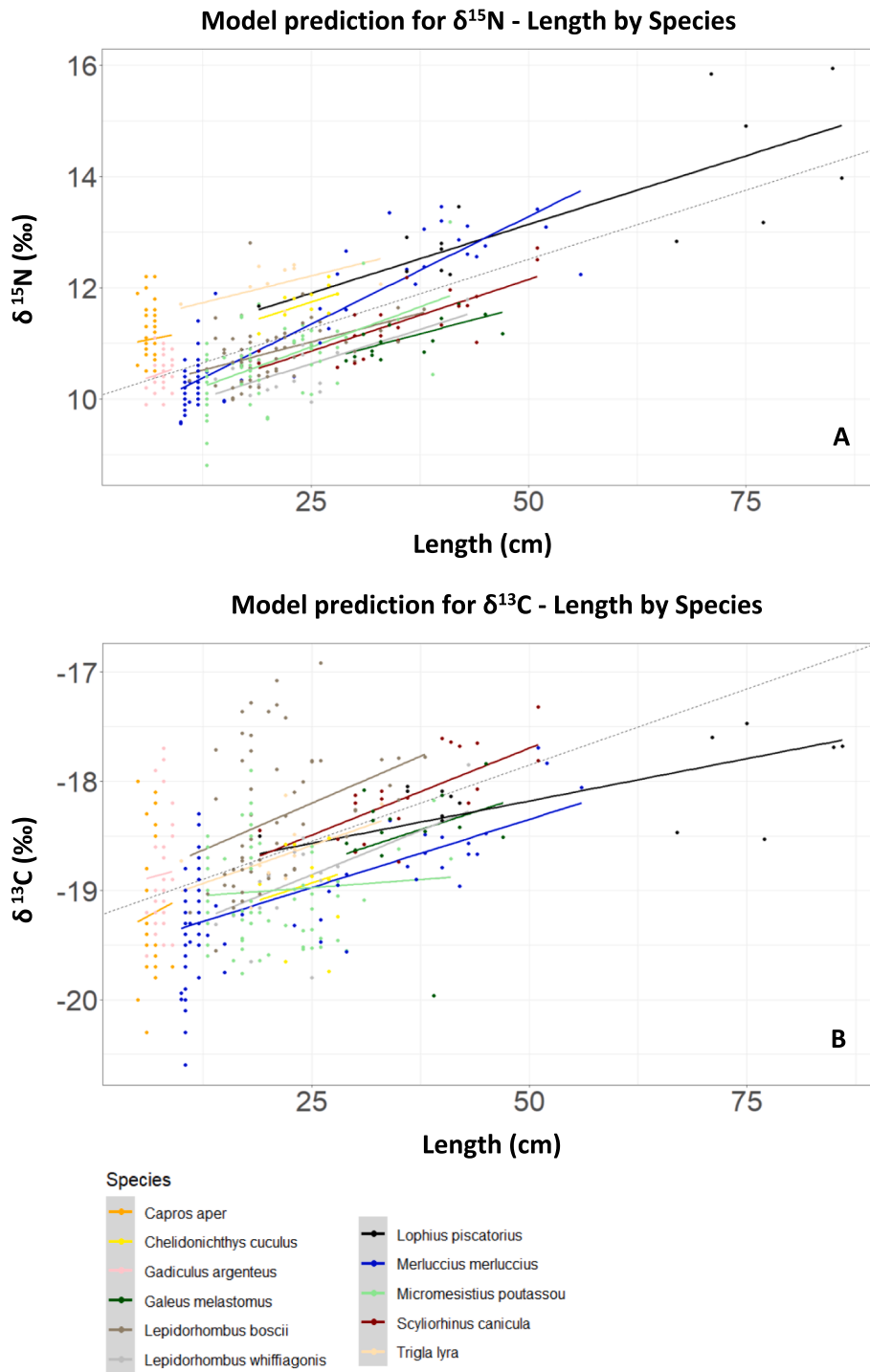


Fig. 2. Isotope value (‰) – Length (cm) predicted specific relation from $\delta^{15}\text{N}$ (A) and $\delta^{13}\text{C}$ (B) Linear mixed model.

3.3. Environmental factors behind baseline isoscapes

Based on the GCV and AIC values of the GAMs, we selected the environmental variables with highest explanatory power to model the $\delta^{13}\text{C}$ and $\delta^{15}\text{N}$ baseline anomalies using GAMs (Supplementary E; F). The final model for the $\delta^{13}\text{C}$ baseline isoscape included Chlorophyll, % OM, Hydrodynamic energy, % Coarse sand and Depth, and explained 30.2% of the deviance. The model for the $\delta^{15}\text{N}$ baseline isoscape included % OM, Depth and % Mud and explained 4.04% of the deviance (Table 2).

Regarding $\delta^{13}\text{C}$ baseline isoscape, Chlorophyll was the variable with

a higher explanatory power (12.47% of deviance explained). $\delta^{13}\text{C}$ baseline anomalies decreased linearly with Chlorophyll concentration, highlighting a strong dependence of the isotopic carbon isoscape with this dynamic variable (Fig. 5a). The same trend was displayed by OM (0.87% of deviance explained), with a linear decrease in $\delta^{13}\text{C}$ baseline anomalies with increasing concentration of OM in the sediment (Fig. 5b). Although Hydrodynamic energy (Fig. 5c), Coarse Sand (Fig. 5d) and Depth (Fig. 5e) were also selected by the model (0.82%, 0.85% and 0.90% of deviance explained respectively), these variables had a negligible effect (p-value > 0.05) on the $\delta^{13}\text{C}$ baseline (Table 2).

In the model of $\delta^{15}\text{N}$ baseline isoscape, only OM showed a marginally

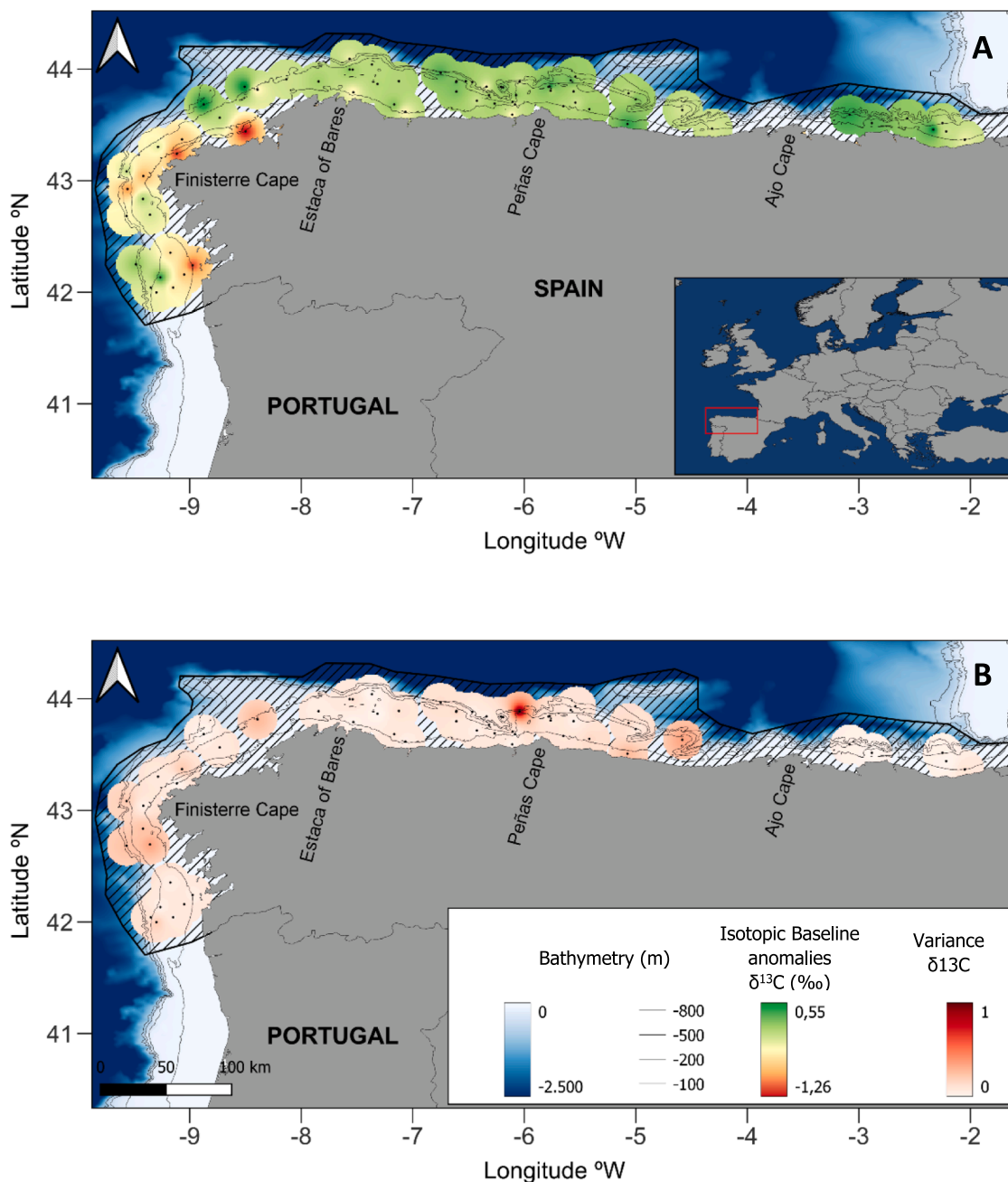


Fig. 3. Results of $\delta^{13}\text{C}$ Linear Model expressed as Baseline anomalies(‰) (A) and Variance (B). *The difference between the number of samples in the anomalies and the variance maps is due to the single data sampling location.

significant effect (2.55% of deviance explained) (Table 2). The effect of %OM on the $\delta^{15}\text{N}$ baseline isoscape was only reliable for a narrow range of %OM values; the model showed a negative trend until reaching values of 3%, thereafter becoming uncertain due to the wide confidence intervals (Fig. 5f). The percentage of Mud (Fig. 5g) and Depth (Fig. 5h) was also selected by the model (1.56% and of deviance explained respectively), but their effect on $\delta^{15}\text{N}$ baseline isoscape was negligible (p-value > 0.05) (Table 2).

4. Discussion

The construction and selection of a suitable baseline is one of the most important steps when using stable isotopes for trophic ecology research (Magozzi et al., 2017). A baseline estimated on the isotopic

signatures of environmental samples or those of the lowest trophic levels of the food web, can be heavily influenced by the environmental variability (Hoefs, 2015) and thus is highly variable in space and time (Vokhshoori et al., 2014). Moreover, baseline estimates based on a single species of the food web, would cause a large deviation and incomplete non-representative results (Post, 2002). In the present study, the multitrophic and multispecies approach offered more robust results, identifying 41.6% of the variability of $\delta^{13}\text{C}$ isotopic signatures and 21.7% of the variability of $\delta^{15}\text{N}$ isotopic signatures of the fish assemblage as driven by the baseline isoscapes.

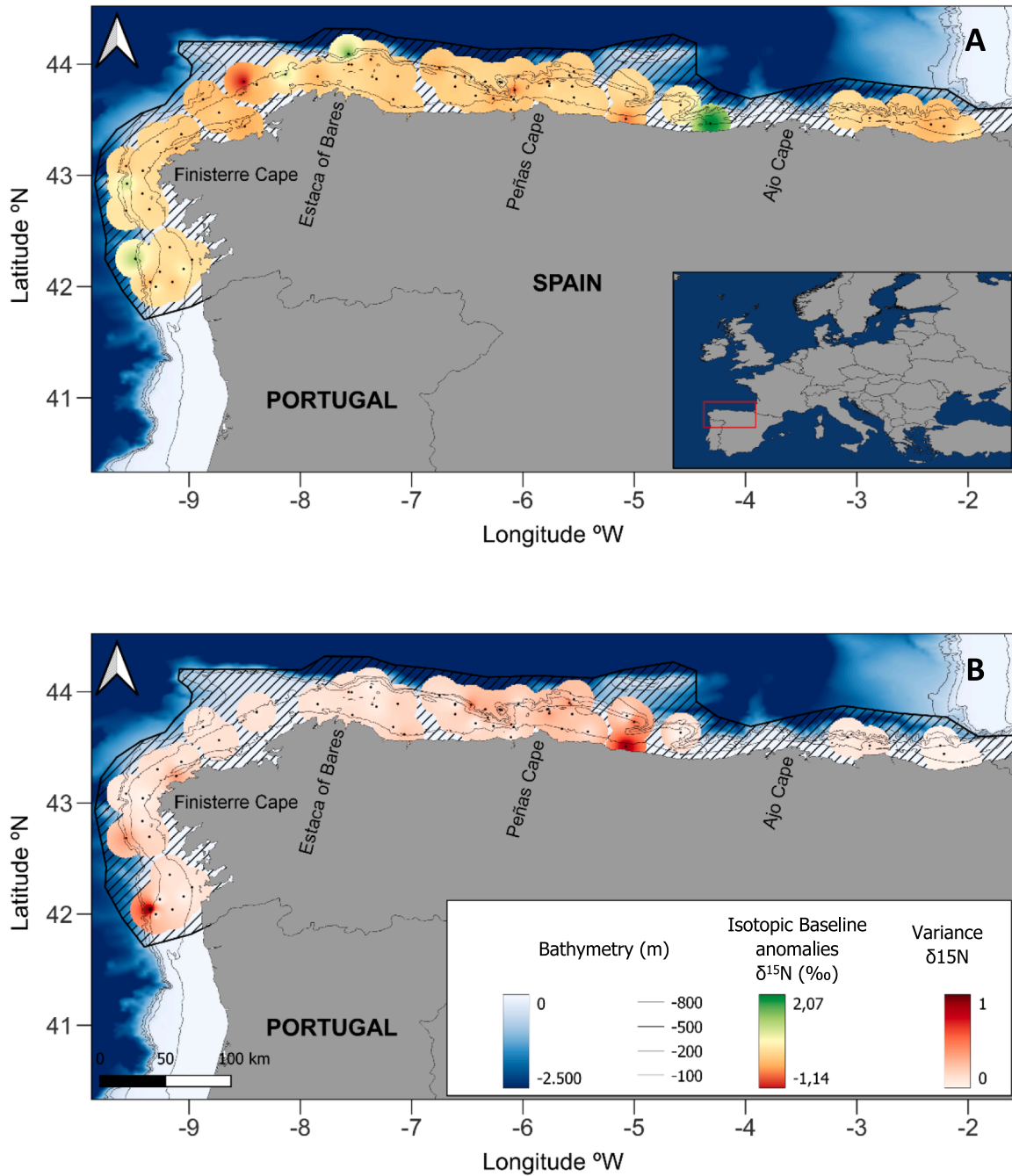


Fig. 4. Results of $\delta^{15}\text{N}$ Linear Model expressed as Baseline anomalies(‰) (A) and Variance (B). *The difference between the number of samples in the anomalies and the variance maps is due to the single data sampling location.

4.1. Estimating baseline isoscapes from community data: Species singularities

To calculate the isotopic baselines upon the community isotopic signatures, we firstly eliminated the biological effect of individual size nested within species, which explained most of the variability in the raw isotopic data. In the scientific literature, the isotopic enrichment with its trophic level is commonly assumed but not so commonly estimated (Hussey et al., 2014). Although most studies assume an increase of between 3 ‰ – 3.4‰ $\delta^{15}\text{N}$ per trophic level (Post, 2002; Navarro et al., 2011), recent research has argued that the nitrogen isotopic enrichment with trophic level might not be linear but incremental, with higher enrichment at the base of the food web and lower within top predators

(Hussey et al., 2014). Our modelling approach, however, is taxonomic, with several of these species undergoing ontogenetic changes in diet during their life span which modify their trophic levels within the ecosystem. Indeed, our results identified a generalised increase in $\delta^{15}\text{N}$ with body size which suggest an increase of trophic level during the species ontogeny. Similar patterns have often been described in the literature for benthic and demersal assemblages (e.g. Jennings et al., 2002; Jennings et al., 2003; MacKenzie et al., 2014), but might not be as obvious for generalist planktivorous fish (Bode et al., 2006). The size increments caused by ontogeny and continued subsequent growth (Galvan et al., 2010) allow predators to increase their potential prey range and their capacity to forage and consume food (Cohen et al., 1993). In our assemblage, *Lophius piscatorius* and *Merluccius merluccius*

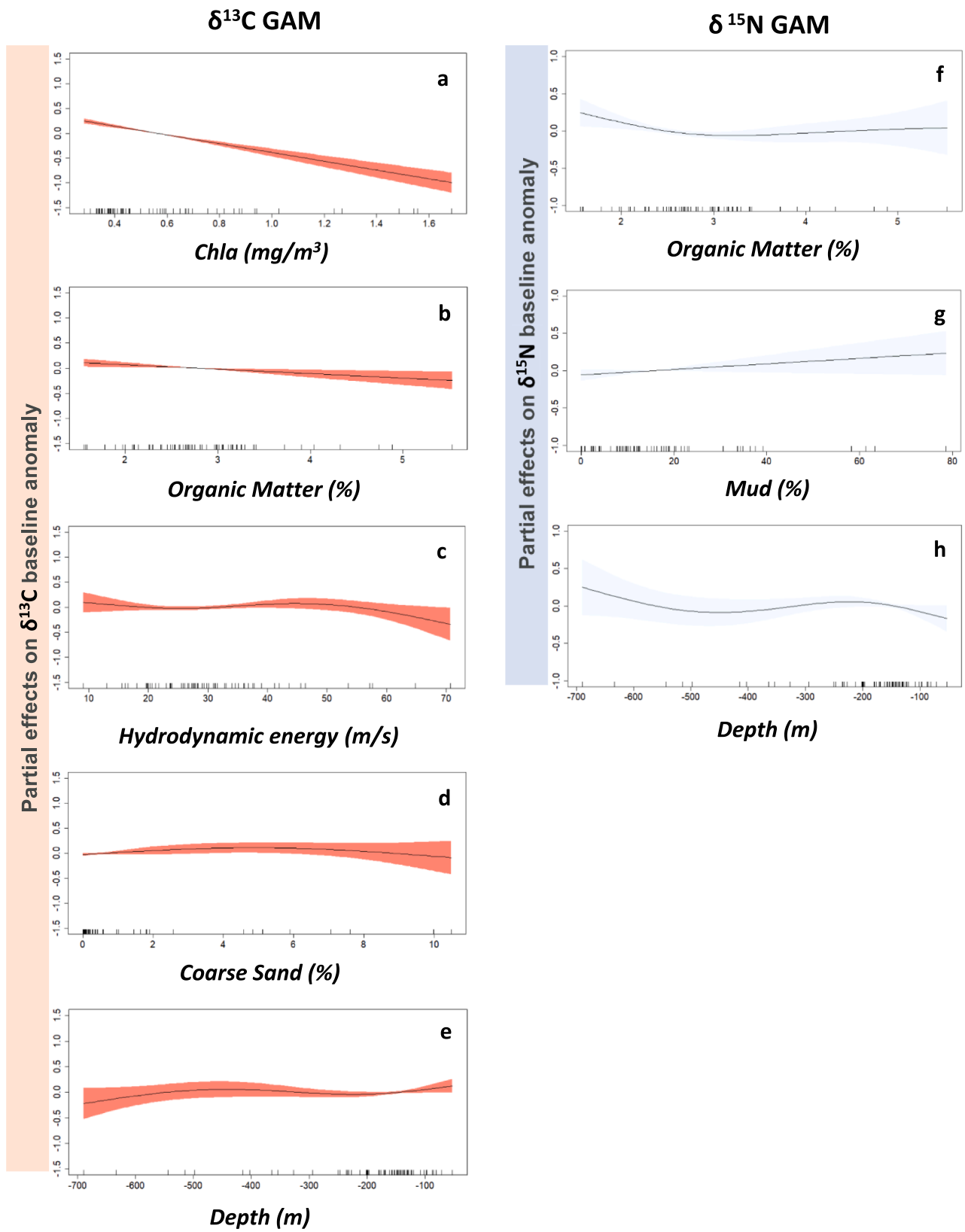


Fig. 5. Results of the GAMs performed using chlorophyll α , organic matter, hydrodynamic energy, sediment type and depth as explanatory variables of changes observed in $\delta^{13}\text{C}$ baseline (left) and $\delta^{15}\text{N}$ baseline (right) anomalies. The variables shown are those selected by the models.

were the demersal species positioned as top predators, particularly at the largest sizes. These species are in fact known to occupy this position in the food web under study (Corrales et al., 2022; Preciado et al., 2015; López-López et al., 2015), but the much steeper increasing trend of $\delta^{15}\text{N}$ in *M. merluccius* indicates that this species undergoes unparalleled changes in diet during their life cycle, from the juvenile to adult, supporting the ontogenetic changes in diet identified in the literature (Velasco and Olaso, 1998). It is also remarkable the high $\delta^{15}\text{N}$ of *Trigla lyra*, a benthic crustacean-feeder (López-López et al., 2011), which positions this species at the top of the benthic food web despite its relatively smaller maximum size. $\delta^{15}\text{N}$ values of *Scyliorhinus canicula*, an opportunistic and scavenger benthic shark (Olaso et al., 2005) at the lower trophic end of the assemblage, could be explained by the content in urea, depleted in $\delta^{15}\text{N}$, in the muscle of elasmobranchs (Logan and Lutcavage, 2010). As expected, the $\delta^{13}\text{C}$ isotopic enrichment along the size ranges of species was weaker than that of $\delta^{15}\text{N}$, and not as homogeneous, as this is commonly estimated around 0.8 ‰ per trophic level in the scientific literature (Zanden and Rasmussen, 2001), but also depends on changes in feeding habitat. Some species could be decreasing their $\delta^{13}\text{C}$, for example, if turning from a benthic-based to a pelagic-based diet promoted by pelagic enrichment in upwelling phenomena (Rooney et al., 2006), and triggering in consequence an spatially heterogeneous enrichment process over the study area. This could be the case of *Micromesistius poutassou* and *Lophius piscatorius* in our assemblage, whose $\delta^{13}\text{C}$ rate of increase with size is sensibly smaller than the rest of the assemblage, may be buffered by lower $\delta^{13}\text{C}$ values in upwelling areas, promoted by the use of the pelagic resource from demersal predators (Rooney et al., 2006).

4.2. Spatial variability in baseline isoscapes and environmental drivers

Our isoscapes identified stronger spatial patterns for $\delta^{13}\text{C}$ than for $\delta^{15}\text{N}$, in agreement with previous studies, which suggest that the carbon isotopic ratio is more strongly influenced by geographic features and oceanographic processes (Ohshimo et al., 2019). Indeed, the carbon isotopic baseline is often highly correlated with primary productivity (Tamelander et al., 2009; Lara et al., 2010; Ho et al., 2021), as trophic fractionation during photosynthesis can vary according to sea surface temperature, the concentration of dissolved CO_2 and the taxonomic composition of the phytoplankton community, which controls its physiology (Magozzi et al., 2017). We identified lower baseline anomalies in the coastal westernmost zone of our study area, the Galician continental shelf, an area characterised by seasonal upwelling of variable intensity and generally higher primary productivity (Gil, 2008; González-Nuevo et al., 2014). Primary productivity in this upwelling region is largely dominated by diatoms (Varela, 1992; Casas et al., 1997), which generally show lower levels of carbon fractionation than smaller phytoplankton groups, driving carbon isoscapes towards more negative $\delta^{13}\text{C}$ values (Popp et al., 1998). While higher values of $\delta^{13}\text{C}$ could also be reflecting a higher influence of benthic trophic pathways or even an input of organic matter from terrigenous origin (Riera and Richard, 1996; Bouillon et al., 2000; Chouvelon et al., 2015 and references therein), this is unlikely to be the main reason driving the baseline isotope anomalies for carbon. Previous studies in the region, could not identify variability in $\delta^{13}\text{C}$ values in the region associated with terrigenous inputs (López-López et al., 2017b). On the contrary, these authors found a remarkable similarity between the isotopic signatures of organic matter in the sediment and in the water column, suggesting a low residence-time of phytodetritus in the water column and rapid sedimentation events characterised by a negligible fractionation. Although there are no large rivers affecting the area (González-Nuevo and Nogueira, 2014) and thus the effect of river runoff is unlikely to influence carbon isoscapes, fine sediments from terrigenous origin have been found to spread several kilometres in the continental shelf in the southernmost region of the study area, outflowing from numerous coastal embayments (López-Jamar et al., 1992). This is also

corroborated by our $\delta^{13}\text{C}$ model which was partly explained by the percentage of organic matter in the sediment, mostly associated with these fine-grained deposits.

Baseline isotope anomalies for $\delta^{15}\text{N}$ displayed larger variability but were more evenly distributed over the study area. The environmental and geographical variables considered only explained a low percentage of the isotope variability. In fact, we expected an effect of primary productivity on the $\delta^{15}\text{N}$ baseline isotope not identified by our results. In upwelling areas, the supplies of deep waters depleted in ^{15}N were expected to leave a footprint on the $\delta^{15}\text{N}$ baseline, which would be rather enriched in this isotope in areas with a higher percentage of recycled production, where the phytoplankton would preferentially incorporate ^{14}N leaving a residual pool of ^{15}N for subsequent production (Montoya, 2007; Chouvelon et al., 2012). In addition, we believed this effect could be augmented by the fact that in pulse production systems, demersal predators tend to rely on pelagic trophic routes when productivity is high (Rooney et al., 2006), engaging in pathways with lower number of trophic levels. On the other hand, under conditions of low productivity, these predators use preferentially benthic trophic pathways, which are structurally more complex in general (Reynolds, 2008), and thus would be expected to achieve higher $\delta^{15}\text{N}$. These processes however are more related to a temporal succession than to a spatial pattern able to persist in time, and thus their effects might be masked by our multitrophic approach, where different species are likely to have distinct isotopic turnovers. In fact, the results of the spatial distribution of $\delta^{15}\text{N}$ isotope were not conclusive.

Regarding the non-significant variables in the models, it is believed that a higher hydrodynamism could contribute to mixing water masses and renewing the carbon and nitrogen pools, that would be enriched under conditions of strong stratification (based on Montoya, 2007). However, we did not find such an effect in our results. Contrary to our expectations, depth was not a significant variable in our models. This variable, which partly correlates with distance to coast, could indicate the prevalence of terrestrial sources of organic matter (Ohshimo et al., 2019), however the small flow of the rivers in our study area (González-Nuevo and Nogueira, 2014) might prevent us from finding such a signal. Depth is also expected to change as the benthic-pelagic coupling weakens, the latter however might be detectable in benthic organisms such as filter-feeding animals (e.g. Jennings et al., 2003; Nerot et al., 2012), but not as relevant for highly mobile demersal fishes. We also included a set of variables related to sediment type (e.g. Kürten et al., 2013a; Espinasse et al., 2022) to provide a detailed substrate spatial description, as we could not rule out a priori an effect of sediment type on isoscapes. Among these variables, the percentage of organic matter in the sediment was the variable with a higher explanatory power, as the isotopic fractionation it undergoes during degradation might change its carbon and nitrogen isotopic signatures. Apparent increases in $\delta^{15}\text{N}$ under high OM loads has been related to bacterial activity, however $\delta^{13}\text{C}$ seems to be less affected by biogeochemical processes but with the isotopic source (Nakatsuka et al., 1997).

4.3. Temporal variability of baseline isoscapes

While our research did not tackle temporal variation in the data, we hypothesise that the lack of spatial variability in the nitrogen baseline across the northern coast of Spain could result from this isotopic baseline displaying high temporal variability. In fact, this would be expected under highly dynamic environments, e.g. those dominated by strong circulatory phenomena (Hoefs, 2015). As the isotopic signature in fish muscle integrates the dietary intake of weeks to months (Vander Zanden et al., 2015; Thomas and Crowther, 2015), it is likely to smooth any short-term variability in the nitrogen isotopic baseline. Our analyses integrated isotopic data obtained in different sampling years and thus, to account for any interannual changes in baseline isoscapes, year was included in the models as a random factor. However, we did not count with a time series and our results regarding interannual variability are

inconclusive. Previous long-term studies in coastal waters have not identified interannual patterns in $\delta^{13}\text{C}$ and $\delta^{15}\text{N}$ isoscapes (McKenzie et al., 2014), but interannual variability in upwelling intensity could be a driver of change for isoscapes at the interannual scale in our study area (López-Lopez et al., 2017). In addition, the $\delta^{13}\text{C}$ isoscape is showing a small but consistent decreasing trend in oceanic waters resulting from the increasing anthropogenic CO₂ in the atmosphere and the consequent ocean–atmosphere balance, known as the Suess effect (Grueber et al., 1999). This effect shows annual decreasing rates between 0.01 and 0.02 ‰ $\delta^{13}\text{C}$ in the North Atlantic (Grueber et al., 1999; Quays et al., 2007), well below our analytical measurement error, and consequently it is unlikely that it could be affecting measurements of isotopic signatures in the demersal fish community.

Our results demonstrated a lack of correlation between the estimated isotopic baseline and the environmental samples measuring the isotopic signature of particulate organic matter in the water column and in the sediment. These results challenge the idea that raw local environmental data are the best baseline to correct animal isotopic signatures. In fact, due to the tissue turnover time in our predators, there is an evident temporal mismatch between the signature of the environmental sample, and that of the fish muscle tissue collected simultaneously. While we can assume the fish community to provide a larger window of isotopic integration, the time that an environmental signal takes to reach a fish predator might differ from few months (seasonal integration) to over a year depending on the species identity, its life cycle stage and its trophic level (Vander Zanden et al., 2015; Thomas and Crowther, 2015). The isotopic signatures of environmental samples, on the contrary, represent the dynamic nature of temporally variable ecosystems, e.g. receiving periodic influxes of nutrients and organic matter, from adjacent systems (Kurlle and McWhorter, 2017; Bode et al., 2020). In addition, demersal predators benefit from both benthic and pelagic food web routes, so they are expected to reflect a mixed baseline at a middle point between the isotopic signatures of these two environments. How much each of these environments contribute to the isotopic signature is also hard to determine, as these predators can switch between feeding routes both seasonally and annually depending on resources availability (Rooney et al., 2006). To overcome the high variability commonly associated with environmental $\delta^{13}\text{C}$ and $\delta^{15}\text{N}$ data, modelling approaches are increasingly used to determine spatial variation of isotopic baselines (Kurlle and McWhorter, 2017; Bosman et al., 2020).

4.4. Final remarks

To our knowledge, this is the first time a multi-trophic and multi-species model has been performed to generate isoscapes based on anomalies. Working with isotopic data of large demersal predators is particularly challenging, as their isotopic signatures integrate benthic and pelagic sources at varied but generally large temporal scales, integrating any potential seasonal variability. As such, the baseline anomalies resulting from our work illustrate the basal signal that remains in the predator tissues, the most temporally stable and prevalent component of spatial isoscapes. Our results validate the use of isotopic signatures at the community level as a robust approach to study marine isoscapes, and suggest a strong link between isotopic baselines and primary production, particularly for $\delta^{13}\text{C}$, highlighting the dynamic nature of marine isoscapes on the continental shelf attending to environmental gradients. However, we discuss here some venues for improving the results of this promising methodological approach. Firstly, monitoring the isotopic signatures of the community with higher temporal resolution and during a larger timespan would allow us to understand annual variability in isotopic baselines (e.g. Espinasse et al., 2022) while applying this approach on a set of species with higher isotopic turnover could provide insights into seasonal isoscape variability. Secondly, the introduction of a more diverse array of species, including other taxa and trophic levels, would better represent the community supporting a more integrative and holistic vision, despite possibly

introducing a higher variability at short temporal scales (Kürten et al., 2013a, b). Thirdly, including additional biological variables in the computation of isoscape anomalies, and/or environmental variables, and interaction between variables particularly those static and dynamic to understand the mechanisms behind the anomalies distributions, which could help us to gain a more throughout understanding of isoscape baseline variability at both spatial and temporal scales. Finally, in a management sense, improving our knowledge on the baseline of food webs is crucial in the development of ecosystem indicators at the medium term. Unravelling the effect of climate change and other anthropogenic factors on the observed changes in the structure and functioning of the ecosystems should be a priority when implementing monitoring programmes to address integrated ecosystem management.

CRediT authorship contribution statement

J.J. Ortiz: Conceptualization, Methodology, Formal analysis, Investigation, Data curation, Writing – original draft, Writing – review & editing. **I. Preciado:** Writing – review & editing, Resources, Investigation, Conceptualization. **M. Hidalgo:** Conceptualization, Resources, Writing – review & editing, Project administration, Funding acquisition. **J.M. González-Irusta:** Conceptualization, Writing – review & editing. **I. M. Rabanal:** Writing – review & editing. **L. López-López:** Conceptualization, Methodology, Formal analysis, Investigation, Resources, Writing – review & editing, Supervision.

Declaration of competing interest

The authors declare that they have no known competing financial interests or personal relationships that could have appeared to influence the work reported in this paper.

Data availability

Data will be made available on request.

Acknowledgements

This study was funded by the COCOCHA project [Grant PID2019-110282RA-I00 funded by MCIN/AEI/ 10.13039/501100011033]. LLL was supported by a contract financed through the “Juan de la Cierva Incorporación 2020” fellowship [IJC2020-043235-I] funded by MCIN / AEI / 10.13039/501100011033 and the European Union “NextGeneration EU/PRTR”. Authors want to acknowledge the rest of the COCOCHA team, and the trophic ecology team at the Spanish Institute of Oceanography (IEO, CSIC) for the collection of isotope samples and the fruitful discussions during the development of this work. Additionally, we are thankful to the scientific staff and the crew of the Demersales surveys without whom this work would not have been possible.

Appendix A. Supplementary data

Supplementary data to this article can be found online at <https://doi.org/10.1016/j.pocan.2024.103205>.

References

- Akaike, H., 1974. A new look at the statistical model identification. *IEEE Trans. Automatic Control* 19 (6), 716–723. <https://doi.org/10.1109/TAC.1974.1100705>.
- Alvarez, I., Gomez-Gesteira, M., DeCastro, M., Lorenzo, M.N., Crespo, A.J.C., Dias, J.M., 2011. Comparative analysis of upwelling influence between the western and northern coast of the Iberian Peninsula. *Cont. Shelf Res.* 31 (5), 388–399. <https://doi.org/10.1016/j.csr.2010.07.009>.
- Barnes, C., Jennings, S., Barry, J.T., 2009. Environmental correlates of large-scale spatial variation in the $\delta^{13}\text{C}$ of marine animals. *Estuar. Coast. Shelf Sci.* 81 (3), 368–374. <https://doi.org/10.1016/j.ecss.2008.11.011>.
- Bartoni, K. (2022). MuMin: Multi-Model Inference. R package version 1.47.1. <http://CRAN.R-project.org/package=MuMin>.

- inferred from the vertical distributions of its $\delta^{15}\text{N}$, $\delta^{13}\text{C}$ and $\delta^{14}\text{C}$. *Deep Sea Res. Part I* 44 (12), 1957–1979. [https://doi.org/10.1016/S0967-0637\(97\)00051-4](https://doi.org/10.1016/S0967-0637(97)00051-4).
- Navarro, J., Coll, M., Louzao, M., Palomera, I., Delgado, A., Forero, M.G., 2011. Comparison of ecosystem modelling and isotopic approach as ecological tools to investigate food webs in the NW Mediterranean Sea. *J. Exp. Mar. Biol. Ecol.* 401 (1–2), 97–104. <https://doi.org/10.1016/j.jembe.2011.02.040>.
- Nerot, C., Lorrain, A., Grall, J., Gillikin, D.P., Munaron, J.M., Le Bris, H., Paulet, Y.M., 2012. Stable isotope variations in benthic filter feeders across a large depth gradient on the continental shelf. *Estuar. Coast. Shelf Sci.* 96, 228–235. <https://doi.org/10.1016/j.ecss.2011.11.004>.
- Ohshimo, S., Madigan, D.J., Kodama, T., Tanaka, H., Komoto, K., Suyama, S., Ono, T., Yamakawa, T., 2019. Isoscapes reveal patterns of $\delta^{13}\text{C}$ and $\delta^{15}\text{N}$ of pelagic forage fish and squid in the Northwest Pacific Ocean. *Prog. Oceanogr.* 175, 124–138. <https://doi.org/10.1016/j.pocean.2019.04.003>.
- Olaso, I., Velasco, F., Sánchez, F., Serrano, A., Rodríguez-Cabello, C., Cendrero, O., 2005. Trophic relations of lesser-spotted catshark (*Scyliorhinus canicula*) and blackmouth catshark (*Galeus melastomus*) in the Cantabrian Sea. *J. Northwest Atl. Fish. Sci.* 35, 481–494.
- Popp, B.N., Laws, E.A., Bidigare, R.R., Dore, J.E., Hanson, K.L., Wakeham, S.G., 1998. Effect of phytoplankton cell geometry on carbon isotopic fractionation. *Geochim. Cosmochim. Acta* 62 (1), 69–77. [https://doi.org/10.1016/S0016-7037\(97\)00333-5](https://doi.org/10.1016/S0016-7037(97)00333-5).
- Post, D.M., 2002. Using stable isotopes to estimate trophic position: models, methods, and assumptions. *Ecology* 83 (3), 703–718. [https://doi.org/10.1890/0012-9658\(2002\)083\[0703:USITET\]2.0.CO;2](https://doi.org/10.1890/0012-9658(2002)083[0703:USITET]2.0.CO;2).
- Preciado, I., Punzón, A., Velasco, F., 2015. Spatio-temporal variability in the cannibalistic behaviour of European hake *Merluccius merluccius*: the influence of recruit abundance and prey availability. *J. Fish Biol.* 86 (4), 1319–1334. <https://doi.org/10.1111/jfb.12642>.
- Preciado, I., Cartes, J.E., Punzón, A., Frutos, I., López-López, L., Serrano, A., 2017. Food web functioning of the benthopelagic community in a deep-sea seamount based on diet and stable isotope analyses. *Deep Sea Res. Part II* 137, 56–68. <https://doi.org/10.1016/j.dsr2.2016.07.013>.
- Puig, P., Company, J.B., Sardà, F., Palanques, A., 2001. Responses of deep-water shrimp populations to intermediate nepheloid layer detachments on the Northwestern Mediterranean continental margin. *Deep Sea Res. Part I* 48 (10), 2195–2207. [https://doi.org/10.1016/S0967-0637\(01\)00016-4](https://doi.org/10.1016/S0967-0637(01)00016-4).
- R Core Team, 2022. R: A language and environment for statistical computing. R Foundation for Statistical Computing, Vienna, Austria <https://www.R-project.org/>.
- Rau, G.H., Sullivan, C.W., Gordon, L.I., 1991. $\delta^{13}\text{C}$ and $\delta^{15}\text{N}$ variations in Weddell Sea particulate organic matter. *Mar. Chem.* 35 (1–4), 355–369. [https://doi.org/10.1016/S0304-4203\(09\)90028-7](https://doi.org/10.1016/S0304-4203(09)90028-7).
- Reynolds, C.S., 2008. A changing paradigm of pelagic food webs. *Int. Rev. Hydrobiol.* 93 (4–5), 517–531. <https://doi.org/10.1002/iroh.200711026>.
- Riera, P., Richard, P., 1996. Isotopic Determination of Food Sources of *Crassostrea gigas* Along a Trophic Gradient in the Estuarine Bay of Marennes-Oléron. *Estuar. Coast. Shelf Sci.* 42 (3), 347–360. <https://doi.org/10.1006/ecss.1996.0023>.
- Rooney, N., McCann, K., Gellner, G., Moore, J.C., 2006. Structural asymmetry and the stability of diverse food webs. *Nature* 442 (7100), 265–269. <https://doi.org/10.1038/nature04887>.
- Sánchez, F., Serrano, A., 2003. Variability of groundfish communities of the Cantabrian Sea during the 1990s. *ICES Mar. Sci. Symp.* 219 (219), 249–260.
- St. John Glew, K., Graham, L.J., McGill, R.A., and Trueman, C.N. (2019). Spatial models of carbon, nitrogen and sulphur stable isotope distributions (isoscapes) across a shelf sea: An INLA approach. *Methods Ecol. Evol.*, 10(4), 518–531. <https://doi.org/10.1111/2041-210X.13138>.
- Tameler, T., Kivimäe, C., Bellerby, R.G., Renaud, P.E., Kristiansen, S., 2009. Base-line variations in stable isotope values in an Arctic marine ecosystem: effects of carbon and nitrogen uptake by phytoplankton. *Hydrobiologia* 630, 63–73. <https://doi.org/10.1007/s10750-009-9780-2>.
- Tanaka, H., Ohshimo, S., Takagi, N., Ichimaru, T., 2010. Investigation of the geographical origin and migration of anchovy *Engraulis japonicus* in Tachibana Bay, Japan: A stable isotope approach. *Fish. Res.* 102 (1–2), 217–220. <https://doi.org/10.1016/j.fishres.2009.11.002>.
- Tenore, K.R., Alonso-Naval, M., Alvarez-Ossorio, M., Atkinson, L.P., Cabanas, J.M., Cal, R.M., Campos, H.J., Castillejo, F., Chesney, E.J., Gonzalez, N., Hanson, R.B., Sanchez, J., Santiago, G., Valdes, L., Varela, M., Yoder, J., 1995. Fisheries and oceanography off Galicia, NW Spain: mesoscale spatial and temporal changes in physical processes and resultant patterns of biological productivity. *J. Geophys. Res. Oceans* 100 (C6), 10943–10966. <https://doi.org/10.1029/95JC00529>.
- Thomas, S.M., Crowther, T.W., 2015. Predicting rates of isotopic turnover across the animal kingdom: a synthesis of existing data. *J. Anim. Ecol.* 84 (3), 861–870. <https://doi.org/10.1111/1365-2656.12326>.
- Trueman, C.N., MacKenzie, K.M., Palmer, M.R., 2012. Identifying migrations in marine fishes through stable-isotope analysis. *J. Fish Biol.* 81 (2), 826–847. <https://doi.org/10.1111/j.1095-8649.2012.03361.x>.
- Vander Zanden, M.J., Clayton, M.K., Moody, E.K., Solomon, C.T., Weidel, B.C., 2015. Stable isotope turnover and half-life in animal tissues: a literature synthesis. *PLoS One* 10 (1), e0116182.
- Varela, M. (1992). Upwelling and phytoplankton ecology in Galician (NW Spain) rias and shelf waters. *Boletín del Instituto Español de Oceanografía*, 8(1), 57–74. <http://pascal-francis.inist.fr/vibad/index.php?action=getRecordDetail&idt=4848102>.
- Velasco, F., Olaso, I., 1998. European hake *Merluccius merluccius* (L., 1758) feeding in the Cantabrian Sea: seasonal, bathymetric and length variations. *Fish. Res.* 38 (1), 33–44. [https://doi.org/10.1016/S0165-7836\(98\)00111-8](https://doi.org/10.1016/S0165-7836(98)00111-8).
- Vokhshoori, N.L., Larsen, T., McCarthy, M.D., 2014. Reconstructing $\delta^{13}\text{C}$ isoscapes of phytoplankton production in a coastal upwelling system with amino acid isotope values of littoral mussels. *Mar. Ecol. Prog. Ser.* 504, 59–72. <https://doi.org/10.3354/meps10746>.
- Waite, A.M., Muhling, B.A., Holl, C.M., Beckley, L.E., Montoya, J.P., Strzelecki, J., Pesant, S., 2007. Food web structure in two counter-rotating eddies based on $\delta^{15}\text{N}$ and $\delta^{13}\text{C}$ isotopic analyses. *Deep Sea Res. Part II* 54 (8–10), 1055–1075. <https://doi.org/10.1016/j.dsr2.2006.12.010>.
- Wood, S.N., 2011. Fast stable restricted maximum likelihood and marginal likelihood estimation of semiparametric generalized linear models. *J. Royal Statist. Soc. (B)* 73 (1), 3–36. <https://doi.org/10.1111/j.1467-9868.2010.00749.x>.
- Zanden, M.J.V., Rasmussen, J.B., 2001. Variation in $\delta^{15}\text{N}$ and $\delta^{13}\text{C}$ trophic fractionation: implications for aquatic food web studies. *Limnol. Oceanogr.* 46 (8), 2061–2066. <https://doi.org/10.4319/lo.2001.46.8.2061>.